New Strontium-based Bioactive Glasses: Physicochemical Reactivity and Delivering Capability of Biologically Active Dissolution Products

Jonathan Lao[†]*, Edouard Jallot*[†]*, and Jean-Marie Nedelec*[‡]

[†] Laboratoire de Physique Corpusculaire, CNRS/IN2P3 UMR 6533, Université Blaise Pascal, 24 avenue des Landais, 63177 Aubière Cedex, France

[‡] Laboratoire des Matériaux Inorganiques, CNRS UMR 6002, Université Blaise Pascal & Ecole Nationale Supérieure de Chimie de Clermont-Fd, 24 avenue des Landais, 63177 Aubière Cedex, France

AUTHOR EMAIL ADDRESSES: lao@clermont.in2p3.fr; jallot@clermont.in2p3.fr; j-marie.nedelec@univ-bpclermont.fr

RECEIVED DATE (to be automatically inserted after your manuscript is accepted if required according to the journal that you are submitting your paper to)

[*]CORRESPONDING AUTHOR:

ABSTRACT: The development of bone tissue regeneration calls for biomaterials able to release biologically active substances in a controlled manner after implantation. In this context, strontium-doped bioactive glasses are of major interest; their key property relies on the increased kinetics of surface reactions, along with the release of critical concentrations of ionic dissolution products capable of stimulating cellular responses. In this paper, we report a complete evaluation of the *in vitro* reactivity of new SiO_2–CaO–SrO and SiO_2–CaO–P_2O_5–SrO bioactive glasses. In contact with simulated acellular physiological fluids, these materials induce the formation of a calcium phosphate surface layer that closely resembles to the biological apatite present in bones. Compared to strontium-free materials, the dissolution of SiO_2–CaO–SrO and SiO_2–CaO–P_2O_5–SrO glasses is reduced. However the surface layer is more quickly transformed into a bone-like apatite phase, according to the kinetics of evolution of the Ca/P atomic ratio. Evidences of the presence of Sr at the glass/biological fluids interface were obtained, along with the demonstration that this element is released in physiological concentrations into the biological environment. Knowing the well-recognized beneficial effects of strontium on cell activity and bone remodeling, this crucial result gives high hopes for the development of innovative applications based on Sr-doped glasses in treatment of osteoporosis and tissue engineering.

MANUSCRIPT TEXT

1 Introduction

In the field of porous inorganic biomaterials research, growing attention is given to the development of biomaterials eligible for loading and/or releasing biologically active substances in a controlled manner.[1] The aim is to achieve a correct biological interaction between the implanted biomaterial and surrounding host tissues. For bone tissue regeneration, biomaterials such as bioactive glasses are of major interest. When put in contact with simulated acellular physiological fluids, bioactive glasses induce the formation of a calcium phosphate interfacial layer that closely resembles to the biological apatite present in bones. But the key property of these biomaterials is that under *in vivo* conditions, i.e. in presence of living bone cells, what is actually obtained at the bioactive glasses' surface is newly formed bone.[2] A major field of applications for bioactive glasses consists of filling small osseous defects, where the rate of tissue generation is of paramount importance. In fact bioactive glasses can actively stimulate bone growth through the release of critical concentrations of ionic dissolution products that cause rapid expression of genes regulating osteogenesis and the production of growth factors.[3] Achieving this requires the perfect tuning of the glass matrix chemical composition. In a previous paper,[4] we proposed new strontium-based bioactive glasses with great potential for bone tissue regeneration and osteoporosis therapy. Indeed several studies underlined the ability of the Sr^{2+} cations to promote bone formation and osteoblasts replication while inhibiting bone resorption by osteoclasts. [5] Recent works also demonstrated enhanced surface adhesion properties for strontium-containing biomaterials.[6] In the present study, we investigate the *in vitro* reactivity of Sr-based bioactive glasses through a complete evaluation of their bioactive properties at both a local and a global scale.

We synthesized mesoporous Sr-doped glasses in the SiO_2–CaO–SrO and in the SiO_2–CaO–P_2O_5–SrO systems using the sol-gel process. *In vitro* interactions with acellular biological fluids were conducted on the prepared materials. The complete follow-up of the biological fluids composition during interaction with bioactive glasses gave access to the materials' global scale reactivity: this allowed 1) supersaturation studies of biological fluids in order to evaluate the potential for each glass to induce the

formation of bone-like apatite, and 2) testing their ability to deliver Sr in physiological concentrations via a controlled leaching of ions. Another point of our study was the collect of reliable quantitative data regarding the *in vitro* dissolution of the material, the ionic exchanges and the formation and growth of the calcium phosphate interfacial layer. The PIXE technique (Particle Induced X-Ray Emission) associated to RBS (Rutherford Backscattering Spectrometry) were employed to record elemental maps of the interface between the bioactive glasses and the biological fluids. The PIXE-RBS nuclear microprobe has sensitivity in the order of a few ppm, which allowed the study of trace elements involved in the bioactivity process. The accurate quantification of major and trace element permitted important evaluation for the kinetics of evolution of the calcium phosphate interfacial layer.

The bioactivity process consists of a well-identified group of physico-chemical reactions occurring at the surface of the material. Briefly, the alkaline and alkaline-earth ions present in the glass matrix are first exchanged with H^+ of the solution, then polycondensation reactions of surface silanols create a high-surface area silica gel. This porous hydrated silica layer provides a large number of sites for the formation and growth of calcium phosphates that will progressively crystallize into a biologically reactive hydroxycarbonate apatite equivalent to the mineral phase of bone.[7] These physico-chemical reactions are common to all the glasses we studied but we will demonstrate that the materials' composition significantly affect the kinetics and amplitude of the phenomena.

1.1 Preparation of the bioactive glass samples

Glasses in the SiO_2–CaO–SrO and in the SiO_2–CaO–P_2O_5–SrO systems were prepared using the sol-gel process. Our samples were labeled using the following convention: glasses named B75–SrX and B67.5–SrX are of chemical composition SiO_2(75 wt.%)–CaO(25-X wt.%)—SrO(X wt.%) and SiO_2(67.5 wt.%)–CaO(25-X wt.%)–P_2O_5(7.5 wt.%)–SrO(X wt.%) respectively, with X = 0, 1, 5 wt %. Tetraethylorthosilicate ($Si(OC_2H_5)_4$), calcium nitrate $Ca(NO_3)_2$,$4H_2O$, strontium nitrate $Sr(NO_3)_2$ and triethylphosphate ($PO(OC_2H_5)_3$) (Sigma-Aldrich) were mixed in ethanol in presence of water and HCl under ambient pressure. The prepared sols were then transferred to an oven at 60°C for gelification and aging. Four hours later, the obtained gels were heated at 125°C for 24 hours, then grinded to powder

and stabilized at 700°C to achieve nitrate elimination and further densification. The corresponding heating schedule was as follows: a furnace was programmed to heat up from room temperature to 700°C with a 10°C/min rate, then the samples were heated at 700°C for 24 hours, and finally they were allowed to cool down to room temperature. Parts of the obtained xerogel powders were compacted into discs of 13 mm diameter and 2 mm height without any additive.

1.2 Materials characterization

Inductively Coupled Plasma-Atomic Emission Spectroscopy (ICP-AES) measurements provided us with the experimental composition of the bioactive glasses (cf. Supporting Information).

Nitrogen gas sorption analyses were performed to characterize the glasses textural properties. The samples were vacuum outgassed at 120°C for 12 hours to remove physically adsorbed molecules such as moisture from the pores. The adsorption/desorption isotherms were recorded on a Quantachrom Autosorb-1 apparatus. The instrument determined isotherms volumetrically by a discontinuous static method at 77K. The surface areas were obtained by applying the BET method to the N_2 isotherm. The pore size distribution was determined by the BJH method on the desorption branch. Total pore volume was measured at a relative pressure P/P_0=0.995. Results are presented in the Supporting Information.

1.3 *In vitro* studies

The glass discs were immersed at 37°C for 1, 6 hours and 1, 2, 5, 10 days in 45 mL of a standard Dulbecco's Modified Eagle Medium (DMEM, Biochrom AG, Germany). DMEM contains inorganic salts, glucose, amino acids and vitamins and is widely used for cell culture. The inorganic salts concentrations in DMEM are almost equal to human plasma. B75, B75-Sr5, B67.5 and B67.5-Sr5 glasses were also studied in the form of glass powder samples: 10 mg of glass particles were soaked at 37°C for 1, 6 h and 1, 2, 3, 4 days in DMEM. In addition, because of the high reactivity of B75 glass particles, *in vitro* assays were conducted on B75 particles at very short times: 15 and 30 minutes soaking in DMEM. For all the glass particles samples, the surface area to DMEM volume ratio was fixed at 500 cm^{-1} per gram of material, taking into account the recommended *in vitro* modeling

conditions.[8] This allows studying the sole influence of the glass matrix composition onto its bioactivity properties, the textural influence being discarded.

After interaction, part of the DMEM was taken to be analyzed with ICP-AES while the glass discs and the glass particles were removed from the solution and air dried. SEM analyses were conducted after different interaction periods to follow up the surface changes and provide us with the same observations that are available in an abundant literature: after soaking, the glasses surface is quickly coated with small calcium phosphate precipitates. Initially limited to some scattered sites, the newly formed surface layer quickly extends over the whole material and the CaP precipitates progressively crystallize by incorporation of anions from DMEM (cf. Ref 4). Before characterization with PIXE-RBS nuclear microprobes, the glass discs and glass particles were embedded in resin (AGAR, Essex, England). Then the glass discs were cut into thin sections of 30 micrometers nominal thickness using a Leica RM 2145 microtome. 1000 nm thin sections of the glass powder samples were prepared by mean of a Leica EM UC6 Ultramicrotome, and laid out on 50 mesh copper grids. Finally the sections and grids are placed on a Mylar film with a hole of 3 mm in the centre. Measurements are performed on the area of the section placed over the hole.

1.4 PIXE-RBS analysis

Chemical mapping of the interface between the glass and the biological medium was performed using the highly sensitive PIXE-RBS nuclear microprobes. The PIXE technique is based on the detection of fluorescence X-rays. The key advantage of the method is the possibility to accurately quantify the elemental concentrations (up to the 10^{-6}g/g level) in user-defined regions of interest. Furthermore the signal-to-noise ratio is a hundred times higher than that of conventional EDXS–electron probe. PIXE and RBS methods are used simultaneously: the PIXE method permits the identification and the quantification of major and trace elements at the biomaterial/biological fluids interface, while RBS is used to determine the electric charge received by the samples during irradiation. This parameter is required for PIXE spectra quantification.

Analyses were carried out at the CENBG (Centre d'Études Nucléaires de Bordeaux-Gradignan, France). The experimental characteristics of the CENBG microbeam line have been published previously in Reference [9]. For PIXE-RBS analyses, we chose proton scanning micro-beam of 1.5 and 2.9 MeV energies for the Sr-free and for the Sr-doped glasses respectively. Such parameter values are needed in view of optimizing the ionization cross-sections and thus the sensitivity for PIXE analyses. The glass discs were probed with a beam which diameter was 2 μm and the intensity was 500 pA. The glass particles samples, which required lower beam intensities because of their thinness, were studied using a 50 pA beam that was focused on a spot of 1 μm. Weak intensities and the choice of protons as the ion beam allowed the target degradation to be minimized during irradiation. However, the intensities were sufficient to permit measurement duration under 1 hour.

An 80 mm^2 Si(Li) detector was used for X-ray detection, orientated at 135° with respect to the incident beam axis and equipped with a beryllium window 12 μm thick. Depending on the type of sample, a set of Al-filters (commonly known as "funny filter") with tiny holes of 500 μm or 2 mm holes drilled at their centre were placed in front of the Si(Li) detector. The "funny filter" allows the detection of heavy trace elements ($Z \geq 25$) whereas it avoids the saturation of the detector by major light ($Z \leq 20$) elements X-rays, since those latter are only detected through the small aperture. PIXE spectra were treated with the software package GUPIX. Relating to RBS, a silicon particle detector was placed at 135° from the incident beam axis and allowed the determination of the number of protons that interacted with the sample. Data were treated with the SIMNRA code. This methodology finally allowed quantifying major and trace elements concentrations.

2 Results

2.1 Chemical mapping of the glass disc/biological fluids interface

The *in vitro* bioactivity properties of B75 and B67.5 glass discs have been already discussed in our previous works[10] and we will use it as a basis for comparison with Sr-doped glasses.

Multielemental maps show that the dissolution of Sr-doped glasses is reduced when compared to undoped samples. Ca maps show that this element is homogeneously distributed after 1 hour of interaction for SiO_2–CaO–SrO glasses, while the release of surface Ca^{2+} had already started at that time for the Sr-free B75. After 6 hours of interaction, B75-Sr1 multielemental maps resembles to those of B75: a Si-Ca-P peripheral layer has formed, and the diffusion of Ca ions from the inner regions up to the glass surface is visible. However for B75-Sr5, B67.5-Sr1, and B67.5-Sr5 Ca is still homogeneously distributed after 6 hours of interaction (cf. Supporting Information), contrary to what was observed for the Sr-free B75 and B67.5. Regarding Sr, it is uniformly during the first 6 h of interaction. Then Sr is partially released from the periphery of B75-Sr1, B75-Sr5, B67.5-Sr1, and B67.5-Sr5.

Sr-doping also influences the development of the peripheral phosphocalcic layer. Presence of P at the glass periphery is detected only after 6 hours for B75-Sr1 and B75-Sr5, while P was detected from the first hour of interaction for B75. Similarly, Mg traces are detected only after 6 hours for SiO_2–CaO–SrO glasses. Thereafter the Ca-P-Mg layer grows at the periphery of SiO_2–CaO–SrO and SiO_2–CaO–P_2O_5–SrO glasses in a way similar to the undoped samples. After 10 days of interaction we observe the same regions that were previously described in Reference [10]. For B75-Sr1 and B75-Sr5, one can distinguish three regions in the glass discs section, depending on the element distributions: *1)* the primary glassy silicate network, where high concentrations of Si are detected, corresponds to the inner region of the glass, *2)* the disc surface, where a Ca-P-rich layer containing Mg and Sr traces has developed on a depth of 10-20 μm, *3)* between those two areas a narrow zone exists that is enriched in Ca; this layer results from the diffusion of the mobile Ca^{2+} from the inner part of the glass to its surface. For B67.5-Sr1 and B67.5-Sr5 as for B67.5, region 3 does not exist, because both phosphate and calcium ions from the primary glass network can migrate to the disc surface.

2.2 Evolution of elemental concentrations at the periphery of the glass discs

The PIXE–chemical maps were divided into various regions of interest using the SUPAVISIO analysis software. Whenever the Ca-P-rich peripheral layers were detected, areas of measurement were created, focusing on the X-ray spectra of these user-defined regions of interest. Then the elemental

concentrations were calculated in these areas. With this methodology, the evolution of elemental concentrations at the glass periphery can be observed and is presented in Figure 1. The results correspond to the average of concentrations calculated in several regions of interest. These regions of interest were defined over various samples in order to be ensured of measurements reproducibility. Each point represents an average of 4 measurements. Errors on elemental concentrations were determined by calculating the quadratic sum of errors related to each measure. They mainly depend on 4 parameters: the statistical error associated to the determination of the elemental peak area, the fit error, the error due to the overlapping peak areas and the errors related to instrumental factors (mainly due to the determination of the electric charge deposited on the samples and due to the irradiation damages).

Figure 1 shows the evolution of elemental concentration at the periphery of the SiO_2–CaO–SrO glasses. The slow evolution of both Si and Ca concentrations at the periphery of Sr-doped glasses indicates a lower amplitude of dissolution for these materials. The higher the Sr concentration in the glass, the slower the Si decrease at the material's periphery. The Ca release is clearly slowed down: the Ca minimum concentration, due to Ca leaching out of the glasses surface, is reached only after 6 h of interaction for B75-Sr1 and after 1 day for B75-Sr5. The Ca minimum value is equal to 15-18 wt % for Sr-doped glasses, which is higher than that of B75: this is another indication on the lower amplitude of dissolution for the Sr-doped glasses.

After the release, the amount of Ca present at the glasses periphery continuously grows; however the increase in Ca concentration is slower for SiO_2–CaO–SrO glasses when compared to B75. After 10 days of interaction, Ca concentration at the Sr-doped glasses peripheries is close to 30 wt %. This is lower than the amount of Ca detected at the periphery of B75 (44 wt %). But we must take into account that B75-Sr1 and B75-Sr5 initially contain lower quantities of Ca. Concerning Si, the peripheries of B75-Sr1 and B75-Sr5 still consist of 6 and 9 % Si respectively after 10 days of interaction.

The trends observed in P concentration are very similar for B75, B75-Sr1, and B75-Sr5. A rapid increase in P concentration occurs and a maximum value is finally reached after 10 days of interaction. P concentration at the peripheries of B75, B75-Sr1, and B75-Sr5 is then close to 12 %. Finally, traces of

Mg are detected in this Ca-P surface layer. Mg concentration increases with immersion time in the biological medium. The amount of Mg incorporated at the periphery of B75-Sr1 and B75-Sr5 is in the order of 1.2 – 1.8 %, and shall be compared to the 0.5 % Mg present at B75 periphery.

Concerning SiO_2–CaO–P_2O_5–SrO glasses, Sr-doping induces similar changes in the materials reactivity (cf. Supporting Information). The evolution of Si and Ca concentrations at B67.5-Sr1 and B67.5-Sr5 peripheries is slowed down when compared to the Sr-free B67.5 glass. After 10 days of interaction, the peripheries of B67.5-Sr1 and B67.5-Sr5 contain higher concentration of Si and lower concentration of Ca than B67.5. P concentration at the materials' periphery is in the same order for all the glasses, while Mg concentration is more important for Sr-doped glasses when compared to the Sr-free glass.

Finally, the evolution of Sr concentration at the periphery of B75-Sr1, B75-Sr5, B67.5-Sr1, and B67.5-Sr5 is visible in Figure 1. Large fluctuations in Sr concentration are observed, resulting from the intense ionic exchange and physico-chemical reactions taking place at the glasses surface. A slight decrease in Sr concentration is visible. The higher the Sr content in the initial glass, the higher the Sr concentration at the material periphery after 10 days of interaction.

2.3 Evolution of elemental concentrations in the inner regions of the glass discs

The elemental concentrations were also calculated in the inner regions of the glass discs that were not directly exposed to the biological fluids (cf. Supporting Information). The migrations of ions from the glassy matrix unto the glass surface cause fluctuations in the chemical composition of the inner parts of the discs. The major changes are observed during the fist 2 days; however after 10 days of interaction, the elemental concentrations are close to their original value. In conclusion, the inner regions of Sr-doped glasses are less modified than that of Sr-free glasses (cf. Reference [10]). The amplitude and kinetics of dissolution are lower for Sr-doped glasses; thus the Ca-P-Mg peripheral layer do not extend up to the inner parts of the materials.

2.4 Composition of biological fluids

Changes in the biological medium composition have been investigated and are presented in Figure 2 for SiO_2–CaO–SrO glasses. Similar results were obtained for SiO_2–CaO–P_2O_5–SrO glasses (cf. Supporting Information). During the early hours of interaction slight variations are observed in Ca concentration. Indeed, the amount of Ca released because of the dealkalinisation of the glasses surface is smaller for Sr-doped glasses. Then, a decrease in Ca concentration is observed with increasing interaction time. After 10 days of interaction, a final increase in Ca concentration had occurred for the Sr-free B75 glass, as a result of the partial dissolution of the Ca-P layer; this final increase is not observed for the Sr-doped glasses. After 10 days of interaction, Ca concentration is equal to 62 ppm for B75-Sr1 and B75-Sr5 glasses, which shall be compared to the 94 ppm Ca for B75. For B67.5-Sr1 and B67.5-Sr5 glasses, Ca concentration is equal to 56 and 49 ppm respectively, whereas it is equal to 67 ppm for the Sr-free B67.5. So there is evidence that higher quantities of Ca are incorporated at the periphery of Sr-doped glasses.

Concerning P concentration in DMEM, it is steadily decreasing with time. The observed trends are similar for all the samples. After 5 days of interaction however, it can be seen that P incorporation at the materials' surface is slowed down for Sr-doped glasses. This could indicate that the glass–DMEM system reaches thermodynamic equilibrium for B75-Sr1, B75-Sr5, B67.5-Sr1, and B67.5-Sr5.

The trends observed for Si concentration in DMEM are very alike for both Sr-free and Sr-doped glasses. As the dissolution reactions break down the glassy network on increasing depths with time, higher concentrations of Si are detected in the biological medium. After 10 days of interaction, Si concentration in the biological medium is lower for Sr-doped glasses. This is another indication on the lower amplitude of dissolution for Sr-doped glasses compared to Sr-free materials.

Figure 2 shows that Sr-doped glasses incorporate more Mg at their surface than other materials. Mg concentration slowly decreases with immersion time; after 10 days, a decrease of 2 ppm has occurred for B75-Sr1 and B75-Sr5, 3 ppm for B67.5-Sr1 and 5 ppm for glass B67.5-Sr5.

Finally, the Sr concentration in DMEM (initially Sr-free) increases up to a few ppm after its release from the glasses surface. It is worth noting that B75-Sr5 and B67.5-Sr5 glasses release 5 times more Sr than B75-Sr1 and B67.5-Sr1, which is in perfect agreement with the initial Sr concentration in these materials.

2.5 Effect of the material shape: *In vitro* bioactivity of glass particles

Bioactive glasses can be implanted either in form of powder or glass bulk: thus we also studied the effect of the material's shape onto its bioactive properties. Our investigation focused on the *in vitro* behaviour of B75-Sr5 and B67.5-Sr5 glass particles.

In a previous paper,[11] we demonstrated that both the glass dissolution and the formation of the Ca-P-Mg layer are faster for B75 glass particles when compared to B67.5 particles. Briefly, B75 induced the formation of a peripheral calcium phosphate layer within a few minutes. But after 6 hours of immersion, this amorphous Ca-P-Mg layer was partially dissolved and after 2 days, it was almost completely removed. The only region remaining was the core of the particles, which is more resistant to dissolution because it is mainly composed of the primary silicate network. For the B67.5 particles, the Ca-P-Mg layer was still present after 2 days of interaction and extended on large regions: after 4 days of interaction with biological medium, B67.5 particles were entirely changed into calcium phosphates that crystallized into an enduring apatite layer.

Concerning the Sr-doped B75-Sr5 and B67.5-Sr5 glasses, the multielemental maps show that Sr-doping significantly slows the material's dissolution and the growth of the peripheral phosphocalcic layer. After 1 hour of interaction, B75-Sr5 has barely begun the incorporation of P coming from the biological environment at its periphery (Figure 3). The release of Ca from the glass surface has also begun. It is only after 6 hours of interaction that the formation of the peripheral calcium phosphate layer is clearly visible. The layer is uniform after 1 day. The core of the material is still composed of the primary silicate network. The Ca-P-Mg layer continuously grows and, unlike the Sr-free B75 glass, it is not dissolved after 4 days of interaction. Figure 3 shows that after 4 days of interaction, the B75-Sr5 particles consist of silicon-enriched calcium phosphates, which contain traces of magnesium and

strontium. The improved stability of B75-Sr5 particles regarding dissolution could be an indication of the formation of an enduring apatite-like phase: once formed at the material's surface, it would act as a protective layer towards dissolution.

Regarding B67.5-Sr5, the glass particles do not seem to have reacted after 6 hours of immersion in the biological medium. After 1 day, little changes have occurred: the Ca release has started and the silicate network is partially broken down on narrow areas at the glass periphery. After 4 days of interaction, B67.5-Sr5 particles still contain a significant amount of Si. Higher Ca and P concentrations are detected at the periphery of the particles; however these elements are extended on thinner regions when compared to the other glasses.

The evolutions of elemental concentrations at the particles' periphery, in the inner part of the particles, and in DMEM, provide us with observations similar to what was noticed for the glass discs. Figure 4 shows the evolution of elemental concentration in the inner part of the glass particles. As stated above, the inner part of B75 particles consists of a silicate network that becomes poorer in Ca with time; on the contrary, for B67.5 the Ca-P-Mg peripheral layer develops to such an extent that even the inner regions of the particles are changed into calcium phosphates. Concerning the Sr-doped glasses, no significant changes are observed in the composition of the inner part of the particles: Sr-doping significantly reduces the dissolution of the material and thus the peripheral Ca-P-Mg layer does not develop to such large areas as B67.5. Concerning the composition of the particles' peripheral layer, higher quantities of Mg are incorporated for the Sr-doped B75-Sr5 and B67.5-Sr5 glasses (cf. Supporting Information). Strontium is partially released from the surface of B75-Sr5 and B67.5-Sr5. After 4 days of interaction, Sr is present in the order of 11 to 15 ppm in the biological medium.

3 Discussion

The previous information will now help us discuss the materials' reactivity at both a local and global scales. Indeed the PIXE analyses provided us with the surface reactivity of glasses (local scale). Studying the Ca/P atomic ratios decrease will permit an evaluation for the kinetics of evolution of the calcium phosphate layer at the glass/biological fluids interface. In addition, the ICP-AES measurements

of the DMEM composition gave us information on their global reactivity. We will use these results to evaluate for each glass the potential of forming a hydroxyapatite layer. This is made possible through supersaturation studies of biological fluids.

3.1 Kinetics of evolution of the Ca-P layer at the glass/biological fluids interface

Amorphous calcium phosphates are often encountered as a transient phase during the formation of insoluble hydroxyapatite (HA): they are usually the first phase that is precipitated from a supersaturated solution containing calcium and phosphate ions.[12] But HA is thermodynamically the most stable and the least soluble of all calcium phosphates at physiological pH.[13] Hence the formation of HA experience a number of kinetics processes, which take place at different rates and involve more than one phosphocalcic phase during the bioactivity mechanism. In this sense, studying the Ca/P atomic ratios at the glasses surface gives essential indication on the evolution of the phosphocalcic layer.

We calculated the Ca/P atomic ratios at the surface of the glass discs by creating thin regions of measurement 1 μm thick at the glass/biological fluids interface. Results are presented in Figure 5. They shall be compared to the 1.67 Ca/P value of $Ca_{10}(PO_4)_6(OH)_2$ stoichiometric HA.

During the first few hours of interaction, the Ca/P atomic ratio is higher for the SiO_2–CaO–SrO glass discs than for SiO_2–CaO. This is because Ca, which is released in lower quantities for the SiO_2–CaO–SrO glass discs when compared to B75, is now present in high concentrations at the surface of the B75-Sr1 and B75-Sr5 glass discs. Beyond 6 hours of interaction, the dissolution and release of Ca are accelerated for B75-Sr1 and B75-Sr5; this, added to the rapid incorporation of P from the biological medium, results in a sharp decrease in the Ca/P ratio at 1 day of interaction. Then, with increasing time of interaction, the Ca/P tends to a value close to the 1.67 value of stoichiometric HA. After 10 days, the Ca/P ratio is equal to 1.8 for glasses B75-Sr1 and B75-Sr5, versus 2.1 for the Sr-free B75. Regarding SiO_2–CaO–P_2O_5–SrO glass discs, the Ca/P atomic ratios are systematically lower than those of B67.5. This is due to *1)* the lower increase in Ca concentration at the periphery of SiO_2–CaO–P_2O_5–SrO glass discs, and *2)* the lower amount of Ca initially present in these materials ─ respectively 24 and 20 wt % for B67.5-Sr1 and B67.5-Sr5, versus 25 wt % for B67.5. After 10 days of interaction, the Ca/P atomic

ratio is closer to that of stoichiometric HA for the Sr-doped B67.5-Sr1 and B67.5-Sr5: 1.6 and 1.7 respectively, versus 1.9 for B67.5.

Concerning the glass particles, the observations are very similar. The Ca/P atomic ratios tends more quickly to the nominal value of stoichiometric HA for the Sr-doped glasses.

In order to establish a comparison between the *in vitro* bioactivity of the different glasses, the kinetics of evolution of the Ca/P ratio were modelled using least squares regression with an exponential law: $R_{Ca/P} = A \cdot \exp\left(-t/\tau\right) + R_{\lim}$, where $R_{Ca/P}$ is the Ca/P value at the glass/biological fluids interface after a period of interaction t, τ is a constant parameter, R_{lim} is the Ca/P asymptotic value, A is the Ca/P amplitude. Indeed we can assume that the Ca/P atomic ratios calculated at the glass surface decrease exponentially with time of immersion in biological fluids, reaching a limit value close to the 1.67 value of HA.

For each sample, Table 1 shows the initial value and the limit of the fitting function at infinity. Modelling the Ca/P decrease allows us to determine the τ parameter: τ represents the speed at which the calcium phosphate layer is transformed into a phosphocalcic phase. Table 1 exhibits the τ values with respect to the SrO content in the initial glass matrix. τ is considerably lower for the Sr-doped glass discs. At the surface of these materials, the calcium phosphate layer evolves more quickly into a phosphocalcic phase. It is worth remembering that, added to these increased kinetics of reaction, the final Ca/P atomic are closer to that of HA for Sr-doped glass discs.

The observations are quite different for the glass particles. Logically, τ is lower for the glass particles, which own small size and porous structure, when compared to the glass discs. But surprisingly, there is no clear evidence of the positive effect of Sr on the material's surface reactivity. The τ values are very alike for the Sr-free B67.5 and the Sr-doped B67.5-Sr5. From the previous micro-PIXE analysis of the glass discs, one can suppose that the calcium phosphate layer is extended on thinner regions at the periphery of Sr-doped glass particles; and even on a depth under the 1µm spatial resolution of the microprobe. Therefore, the evaluation of the Ca/P atomic ratios could be distorted for the glass particles.

3.2 Changes in the degree of supersaturation in DMEM

Intense ionic exchanges occur at the bioactive glasses' surface that cause major changes in the supersaturation degree for HA formation in biological fluids. Thus the potential for each glass to form an apatitic layer can be extrapolated from the corresponding evolution of the supersaturation degree. [12] The supersaturation degrees were calculated by considering the formation of stoichiometric HA. Observing the evolution trends for the supersaturation degree will allow the comparison for the *in vitro* bioactivity of each glass.

Given the formation equilibrium of HA ($10Ca^{2+} + 6PO_4^{3-} + 2OH^- \leftrightarrow Ca_{10}(PO_4)_6(OH)_2$), the ionic activity product is defined as: $Q = \gamma_{Ca^{2+}}{}^{10} \cdot [Ca^{2+}]^{10} \cdot \gamma_{PO_4^{3-}}{}^{6} \cdot [PO_4^{3-}]^6 \cdot \gamma_{OH^-}{}^{2} \cdot [OH^-]^2$, where γ_i is the activity coefficient. The activity coefficients have been determined in previous works:[14] for a solution at physiological ionic strength γ_i is equal to 0.36 for Ca^{2+}, 0.06 for PO_4^{3-} and 0.72 for OH^-. Therefore the ionic activity product Q can be calculated because Ca and P concentrations were measured, while the amount of hydroxyl ions was deduced from pH measurements.

The supersaturation degree for HA formation in the solution is defined as: $SD = Q / K_{sp}$, where K_{sp} is the solubility product of HA in aqueous solution. K_{sp} is reported to be $10^{-117.2}$ at 37 ° C. [13, 15] Then it is possible to determine the evolution of the system considering that it tends to thermodynamic equilibrium. The solution and the HA mineral phase reach equilibrium when SD =1. For SD < 1, dissolution of the HA mineral is favoured. For SD >1, the solution is supersaturated with respect to the HA mineral and precipitation of HA is favoured.

Figure 4 shows the evolution of SD in DMEM for both glass discs and glass particles. It is well known that body fluids are initially supersaturated with respect to HA under normal condition. [16] Thus HA precipitation is encouraged and will preferentially occur on the bioactive glasses surfaces: they provide favourable sites for HA nucleation, especially because low interfacial energies are granted by the development of a silica gel on the surface of the glasses (3rd stage of the bioactivity process). [14] During the first times of interaction, an increase in SD occurs because of the release of Ca^{2+} ions from

the glass matrix. After the dealkalinisation of the glass surface, *SD* decreases with increasing time of interaction: Ca^{2+}, PO_4^{3-} and OH^- are incorporated at the glass surface, supplying the HA mineral growth. Different behaviours are observed, depending on the glass type. SD decreases more quickly for SiO_2–CaO–SrO and SiO_2–CaO–P_2O_5–SrO glasses when compared to the Sr-free glasses. From a thermodynamic concern, Sr-doped glasses demonstrate a greater potential for the *in vitro* formation of hydroxyapatite precipitates at their surface.

Concerning the glass particles, the supersaturation degrees exhibit similar evolution (Figure 4). For B75 glass particles, SD decreases rapidly after the dealkalinization stage and then a limit value is reached after 1 day of interaction: the evolution of the system is then suspended between 1 and 3 days. After 4 days SD increases, indicating the dissolution of the HA mineral phase previously formed. B75-Sr5 particles behave in a different way. Although the evolution of SD is slowed down after 1 day of interaction, SD steadily decreases for B75-Sr5. In a way similar to what was observed for the glass discs, the P-containing glass particles exhibit higher decrease slopes. In addition, the evolution of the glass–biological fluids system is quicker for the Sr-containing B67.5-Sr5 than for B67.5. From a thermodynamic concern, B67.5, B67.5-Sr5, and B75-Sr5 glass particles own the greatest potential for the formation of HA. However many other parameters shall be given consideration in evaluating the *in vitro* bioactivity; it is thus essential to compare these results with the micro-PIXE analysis of the materials.

3.3 Local and global reactivity of the bioactive glasses

The effect of Sr^{2+} onto the glasses reactivity can be summed up as: 1) the dissolution of Sr-doped glasses is reduced compared to the Sr-free glasses; 2) the calcium phosphate layer is thinner at the periphery of Sr-doped glasses, and 3) the Ca/P atomic ratio indicates that the layer is more quickly changed into an apatitic mineral, in which higher concentrations of Mg are incorporated. Let us now develop these three points.

1) Reduced dissolution

The reduced dissolution of Sr-doped glasses is stated by the micro-PIXE analysis of the materials' surface which demonstrates the Ca release is delayed. This is confirmed by measurements of the DMEM composition: during the first hours of interaction, lower quantities of Ca are leached into the medium for Sr-doped glasses. Moreover, the evolution of Si and Ca concentrations is slowed down at the periphery of the Sr-containing materials.

2) Thinner Ca-P layer

There is evidence that the apatite-like layer is thinner at the periphery of Sr-doped materials: during the first times of interaction, the surface layer of Sr-doped glasses consists of higher quantities of Si and lower quantities of Ca when compared to the Sr-free materials. Indeed, the dissolution of Sr-doped glasses being reduced, the Ca-P surface layer cannot grow onto such large areas as for the Sr-free glasses. This is particularly visible for the glass particles: lower concentrations of Ca and P are detected at the periphery of B75-Sr5 and B67.5-Sr5 particles, while high concentrations of Si still remain. For the Sr-doped glass particles, the calcium phosphate layer could develop on such thin regions that the presence of HA nanocrystals could not be detected with a 1 μm PIXE probe.

3) Enhanced bioactivity

For the Sr-doped glass discs the Ca/P atomic ratio indicates that the calcium phosphate layer is more quickly changed into an apatite-like mineral. This explains why the peripheral Ca-P layer is not dissolved for B75-Sr5 glass particles, contrary to what was observed for B75: an enduring apatitic layer, resistant to dissolution, is formed.

These observations can be related to the physicochemical properties of the glass matrices' elements. The amount of Ca in the Sr-doped glasses is initially lower, the Ca cations being substituted by Sr^{2+}. Both Ca and Sr are alkaline-earth elements and act as network modifiers in the silicate structure. However Table 2 investigates the ionic radius, ionic field strength, coordination type, single bond strength with oxygen and electronegativity of Ca and Sr cations, and some interesting differences are shown. In particular, the M−O bond strength is higher for Sr^{2+}; thus the ability of $Sr^{2+}$to be exchanged

with H^+ from the solution (first stage of the bioactivity process) will be reduced when compared to Ca^{2+}, and the dissolution kinetics of the Sr-doped materials are modified. Another point going that way is that the electronegativity of Sr is lower than that of Ca: in the glassy network, the $\left(-\!\!\!\diagup\!\!\!\diagdown Si-O^-\right)Sr^{2+}$ bond is therefore more stable due to a more balanced distribution of electronic charges. Hence the reduced dissolution of Sr-doped glasses, which own a lower reservoir of Ca than Sr-free glasses, results in a limited deployment of the phosphocalcic layer.

On the other hand, the Ca-P layer is more quickly changed into an apatitic layer for Sr-doped glasses. Therefore, more Ca^{2+}–Mg^{2+} substitutions are made possible within the newly formed apatitic layer for Sr-doped glasses. This is why larger quantities of Mg are detected at the surface of these materials. The presence of appreciable amounts of Mg at the glass/biological fluids interface is important because of its well-recognized bactericidal and anti-inflammatory properties. [17]

Finally, the most remarkable properties of SiO_2–CaO–SrO and SiO_2–CaO–P_2O_5–SrO glasses are the presence of Sr within the newly formed Ca-P-Mg surface layer, coupled with the release of Sr traces into the biological environment. Indeed the final Ca/Sr atomic ratios at the glasses surface have been calculated for each samples and range from 20 to 180, depending on the initial Sr content in the material. Furthermore, Sr is partially released from the glasses surface into the initially Sr-free biological medium. After 10 days of interaction, 1 to 6 ppm Sr is released from the glass discs, and 11 to 15 ppm Sr from the glass particles. Such Sr quantities are very attractive for antiosteoporotic applications, because they are in the same order of magnitude than those measured *in vivo* in plasmas of animals treated with Sr-based drugs (i.e. strontium ranelate) which were found to have obvious anti-osteoporotic effects:[18] namely, the stimulation of osteoblasts differentiation, an increase in bone formation, along with a decrease in bone resorption.[19] Glasses doped with 5 % Sr deliver 5 times more Sr than glasses doped with 1 %: so there is evidence that the delivered dose of Sr can be controlled through a fine tuning of the materials composition. This is an essential result in view of further clinical applications in bone regeneration and osteoporosis therapy.

4 Conclusion

The influence of strontium onto the bioactive properties of SiO_2–CaO–SrO and SiO_2–CaO–P_2O_5–SrO glasses has been highlighted at both a local and a global scale. The ability of Sr-doped glasses to deliver Sr in physiological concentrations at the material surface and within the medium via a controlled leaching of ions has been successfully evaluated.

Doping with Sr reduces the material's dissolution and the growth of the newly formed phosphocalcic surface layer. Nevertheless, the surface layer is more quickly transformed into an HA-like phase, according to the kinetics of evolution of the Ca/P atomic ratio. Evidences of the presence of Sr at the glass/biological fluids interface were obtained, along with the demonstration that this element is released in physiological concentrations into the biological environment. Knowing the well-recognized beneficial effects of strontium on cell activity and bone remodeling, this crucial result gives high hopes for the development of innovative applications based on Sr-doped glasses in treatment of osteoporosis and tissue engineering. Aiming at this, cellular studies will soon be completed that investigate the capability of these materials to promote the bone cells activity.

ACKNOWLEDGMENT: This work was supported by ANR in the National Program of Nanosciences and Nanotechnologies PNANO2005 (project "BIOVERRES" n° ANR-05-NANO-040). Philippe Moretto and the AIFIRA team are gratefully acknowledged for their help with PIXE-RBS measurements at the CENBG.

SUPPORTING INFORMATION AVAILABLE: Experimental composition of the glasses, N_2 sorption analyses (BET surface area, average and modal pore diameters and total pore volume), Distribution of elements at the interface between the SiO_2–CaO–SrO and SiO_2–CaO–P_2O_5–SrO glass discs and biological fluids after 6 hours of interaction, Evolution of elemental concentrations at the periphery of the SiO_2–CaO–P_2O_5–SrO glass discs, Evolution of elemental concentrations in the inner

regions of the glass discs, Evolution of elemental concentrations at the periphery of the glass particles, Composition of biological fluids during interaction with the glass particles.

FIGURE CAPTIONS

Figure 1. Evolution of elemental concentrations at the periphery of SiO_2–CaO–SrO glass discs with time of interaction with biological fluids.

Figure 2. Evolution of elemental concentrations in biological fluids with time of interaction with SiO_2–CaO–SrO glass discs.

Figure 3. Chemical mapping at the periphery of B75 and B75-Sr5 glass particles after 1 hour and 4 days of interaction with biological fluids.

Figure 4. Evolution of elemental concentrations in the inner regions of the glass particles with time of interaction with biological fluids.

Figure 5: Evolution of the Ca/P atomic ratio at the glasses surface as a function of interaction time. For B75 glass particles, the Ca/P atomic ratio is considered to be not available beyond 6 hours of interaction because of the dissolution of the Ca-P layer.,

Figure 6. Evolution of the supersaturation degree for hydroxyapatite (HA) formation in biological fluids with time of interaction with glass discs and glass particles, −◆−B75, - - ■- - B75-Sr1, ····▲···· B75-Sr5, −◇− B67.5, - - □- - B67.5-Sr1, · ·△· · B67.5-Sr5

FIGURES:

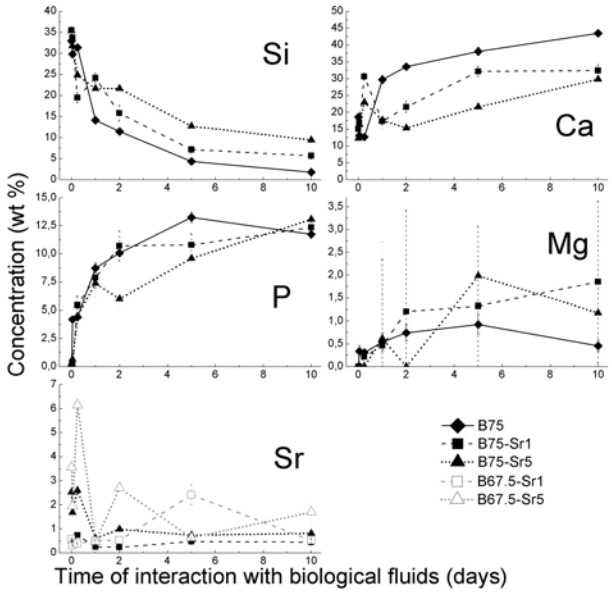

Figure 1

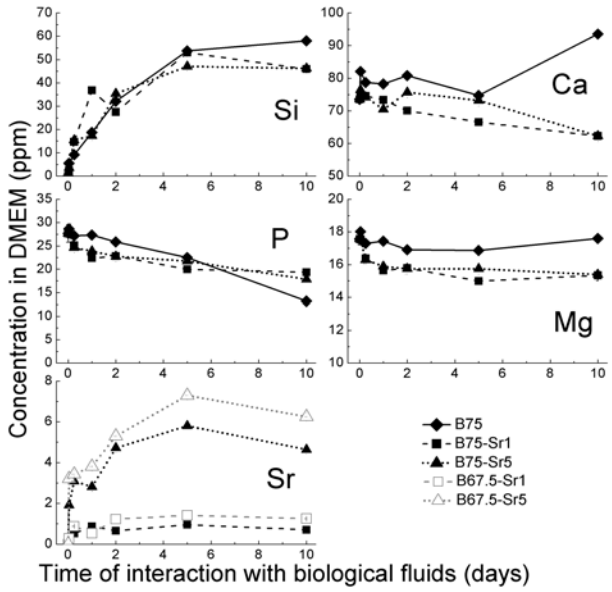

Figure 2

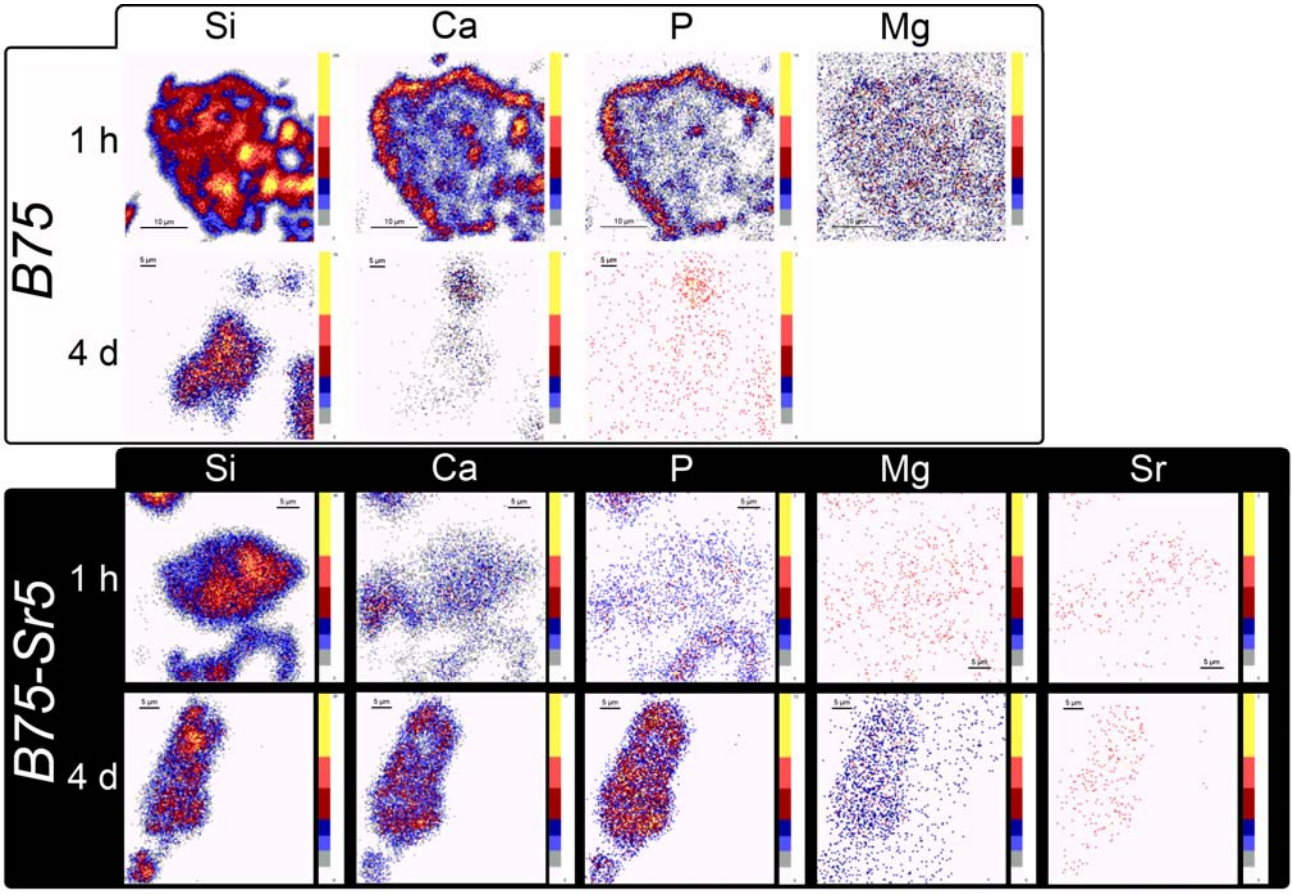

Figure 3

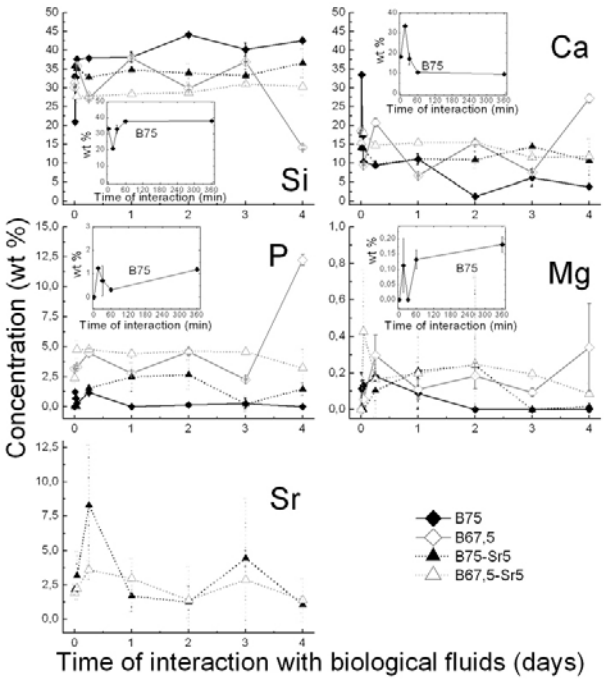

Figure 4

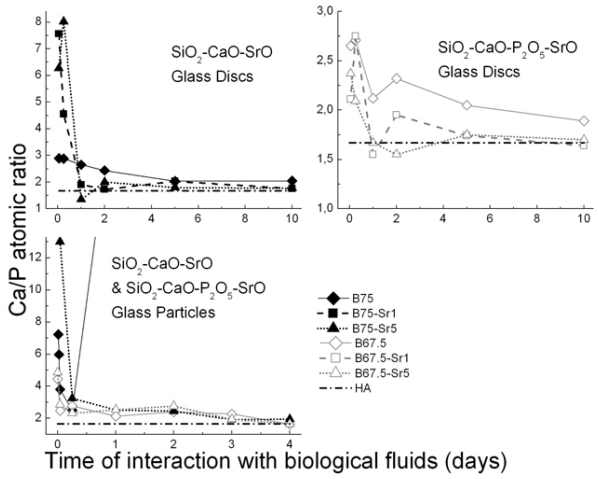

Figure 5

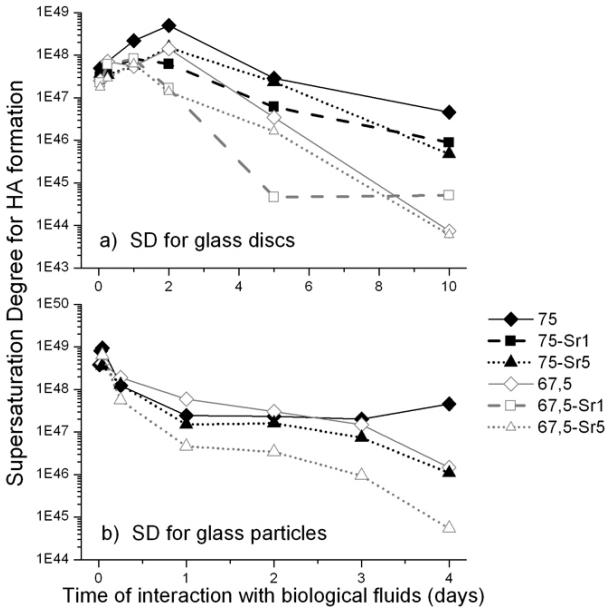

Figure 6

TABLES.

		Modelling : $R_{Ca/P} = A \cdot \exp\left(-\frac{t}{\tau}\right) + R_{\lim}$		*Ca/P experimental*		
		Initial value t = 1 hour	Limit t = ∞	Initial value [a] t = 1 hour [b] t = 15 min	Final Value [c] t = 10 days [d] t = 4 days	***τ parameter (hours)***
GLASS DISCS	B75	2.95	1,99	2.89 [a]	2.05 [c]	**58.9**
	B75-Sr1	8.51	1.81	7.56 [a]	1.76 [c]	**6.6**
	B75-Sr5	7.87	1.55	6.26 [a]	1.77 [c]	**15.6**
	B67.5	2.70	1,96	2.65 [a]	1.89 [c]	**36.9**
	B67.5-Sr1	2.43	1.70	2.11 [a]	1.64 [c]	**20.7**
	B67.5-Sr5	2.47	1.66	2.37 [a]	1.70 [c]	**8.5**
GLASS PARTICLES	B75	9.67	–	7.23 [b]	–	**N/A**
	B75-Sr5	13.05	2.05	13.01 [a]	1.95 [d]	**2.1**
	B67.5	4.43	1.90	4.43 [a]	1.64 [d]	**0.5**
	B67.5-Sr5	4.85	1.85	4.86 [a]	1.64 [d]	**0.7**

Table 1. Ca/P initial values, final experimental values, limits of the fitting function at infinity and τ parameter values for all the materials. For B75 particles, the τ parameter is considered to be not available (N/A) because of the final dissolution of the Ca-P layer.

	Coordination type	Ionic radius (Å)	Ionic field strength Z/r^2 ($Å^{-2}$)	Electronegativity	M–O bond strength (kJ/mol)
Ca^{2+}	VI	0,99	2,04	1,04	351
Sr^{2+}	VI	1,18	1,44	0,99	389

Table 2. Coordination type, Shannon ionic radius, ionic field strength, Allred–Rochow electronegativity, and single bond strength with oxygen of Ca and Sr cations. [20]

REFERENCES.

[1] Vallet-Regí, M. *Chemical Engineering Journal* **2008,** 137, 1.

[2] (a) Hench, L. L. *J. Am. Ceram. Soc.* **1998,** 81, 1705. (b) Yuan, H.; De Bruijn, J.D.; Zhang, X.; Van Blitterswijk, C.A.; De Groot, K. *J. Biomed. Mater. Res.* **2001**, 58, 270. (c) Livingston, T., Ducheyne, P. Garino, J. *J. Biomed. Mater. Res.*, **2002**, 62, 1. (d) Yli-Urpo, H., Lassila, L.V.J., Naerhi, T.O., Vallittu, P.K. *Dent. Mater.*, **2005**, 21, 201.

[3] Hench, L. L.; Polak, J. M. *Science* **2002,** 295, 1014.

[4] Lao, J.; Jallot, E.; Nedelec, J.-M. *Chem. Mater.* **2008,** 20, 4969.

[5] (a) Marie, P. J. *Bone* **2007,** 40, S5. (b) Meunier, P. J.; Roux, C.; Seeman, E.; Ortolani, S.; Badurski, J. E.; Spector, T. D.; Cannata, J.; Balogh, A.; Lemmel, E. M.; Pors-Nielsen, S.; Rizzoli, R.; Genant, H. K.; Reginster, J. Y. *N Engl J Med* **2004,** 350, 459.

[6] Xue, W.; Moore, J. L.; Hosick, H. L.; Bose, S.; Bandyopadhyay, A.; Lu, W. W.; Cheung, K. M.; Luk, K. D. *J Biomed Mater Res A* **2006,** 79, 804.

[7] Ohura, K.; Nakamura, T.; Yamamuro, T.; Kokubo, T.; Ebisawa, Y.; Kotoura, Y.; Oka, M. *J Biomed Mater Res* **1991,** 25, 357.

[8] Jones, J. R.; Sepulveda, P.; Hench, L. L. *J Biomed Mater Res* **2001,** 58, 720.

[9] Incerti, S.; Zhang, Q.; Andersson, F.; Moretto, P.; Grime, G. W.; Merchant, M. J.; Nguyen, D. T.; Habchi, C.; Pouthier, T.; Seznec, H. *Nucl. Instr. Meth. B* **2007,** 260, 20.

[10] (a) Lao, J.; Nedelec, J. M.; Jallot, E. *J. Phys. Chem. C* **2008,** 112, 9418. (b) Lao, J.; Nedelec, J. M.; Moretto, P.; Jallot, E. *Nucl. Instr. Meth. B* **2007,** 261, 488. (c) Lao, J.; Nedelec, J. M.; Moretto, P.; Jall, E. *Nucl. Instr. Meth. B* **2006,** 245, 511.

[11] Lao, J.; Nedelec, J.-M.; Moretto, P.; Jallot, E. *Nucl. Instr. Meth. B* **2008,** 266, 2412.

[12] Yan, X.; Huang, X.; Yu, C.; Deng, H.; Wang, Y.; Zhang, Z.; Qiao, S.; Lu, G.; Zhao, D. *Biomaterials* **2006,** 27, 3396.

[13] Dorozhkin, S. V. *J. Mater. Sci.* **2007,** 42, 1061.

[14] Ohtsuki, C.; Kokubo, T.; Yamamuro, T. *J. Non-Cryst. Sol.* **1992,** 143, 84.

[15] (a) Fernandez, E.; Gil, F. J.; Ginebra, M. P.; Driessens, F. C. M.; Planell, J. A.; Best, S. M. *J. Mater. Sci. Mater. Med.* **1999,** 10, 169. (b) Fernandez, E.; Gil, F. J.; Ginebra, M. P.; Driessens, F. C. M.; Planell, J. A.; Best, S. M. *J. Mater. Sci. Mater. Med.* **1999,** 10, 177.

[16] Neuman, W.; Neuman, M. In *The Chemical Dynamics of Bone Mineral;* CAN 52:30466 AN 1958:30466 CAPLUS, Publisher: Univ. Press, Chicago, 1958; pp 34.

[17] (a) Almoznino-Sarafian, D.; Berman, S.; Mor, A.; Shteinshnaider, M.; Gorelik, O.; Tzur, I.; Alon, I.; Modai, D.; Cohen, N. *Eur J Nutr* **2007,** 46, 230. (b) Weglicki, W. B.; Phillips, T. M.; Freedman, A. M.;

Cassidy, M. M.; Dickens, B. F. *Mol Cell Biochem* **1992,** 110, 169. (c) Rijkers, G. T.; Henriquez, N.; Griffioen, A. W. *Magnes Res* **1993,** 6, 205.

[18] Dahl, S. G.; Allain, P.; Marie, P. J.; Mauras, Y.; Boivin, G.; Ammann, P.; Tsouderos, Y.; Delmas, P. D.; Christiansen, C. *Bone* **2001,** 28, 446.

[19] Grynpas, M. D.; Hamilton, E.; Cheung, R.; Tsouderos, Y.; Deloffre, P.; Hott, M.; Marie, P. J. *Bone* **1996,** 18, 253.

[20] (a) Weast, R.C. In *CRC Handbook of Chemistry and Physics*, 56th Ed., Publisher: CRC Press, Ohio, 1976. (b) Brewer, L.; Brackett, E. *Chem. Rev*., **1961**, 61, 425. (c) Gingerich, K.A.; Cocke, D.L. *J. Chem. Soc. Chem. Commun*. **1972**, 9, 536. (d) Shannon D. *Acta Crystallographica* **1976**, A 32, 751.